RSC Advances

This is an *Accepted Manuscript*, which has been through the Royal Society of Chemistry peer review process and has been accepted for publication.

Accepted Manuscripts are published online shortly after acceptance, before technical editing, formatting and proof reading. Using this free service, authors can make their results available to the community, in citable form, before we publish the edited article. This *Accepted Manuscript* will be replaced by the edited, formatted and paginated article as soon as this is available.

You can find more information about *Accepted Manuscripts* in the Information for Authors.

Please note that technical editing may introduce minor changes to the text and/or graphics, which may alter content. The journal's standard Terms & Conditions and the Ethical guidelines still apply. In no event shall the Royal Society of Chemistry be held responsible for any errors or omissions in this *Accepted Manuscript* or any consequences arising from the use of any information it contains.

ROYAL SOCIETY OF CHEMISTRY

www.rsc.org/advances

Modelling and analysis on the effect of different parameters on a parabolic-trough concentrating solar system

M.K. Islam[*,a], M. Hasanuzzaman[a], N.A. Rahim[a,b]
[a]UM Power Energy Dedicated Advanced Centre (UMPEDAC), Level 4, Wisma R&D, University of Malaya, 59990 Kuala Lumpur, Malaysia
[b] Renewable Energy Research Group, King Abdulaziz University, Jeddah 21589, Saudi Arabia

Abstract

Concentrating solar power technologies are potential energy-harvesting systems. This paper simulates and analyzes the design of a parabolic-trough concentrating solar system. Optimum measurements are sought for the receiver, and collector performance is investigated using three heat transfer fluids, namely, ammonia, nitrogen, and carbon dioxide. Receiver parameters are optimized to achieve the maximum thermal efficiency of the collector. The concentration ratio, collector aperture area, and mass flow rate of the fluids significantly influenced the collector's efficiency and the heat removal factor.

Keywords: Energy, Solar energy, Parabolic trough, Receiver, Collector efficiency.

1. Introduction

Increases in population and wealth has led to greater energy consumption. Soaring oil prices, limited non-renewable resources, increased environmental awareness, and abundant renewable resources drew attention from all nations to take initiatives in utilizing renewable energy [1-6]. Solar is among the renewable energy sources with the most potential. Solar energy can be intercepted and focused onto small receiving areas that can be exploited by a concentrating system. A concentrating system is beneficial for its low cost design, as well as the availability of components such as mirrors, receiver tubes, and compatible integration with fossil fuel technologies to form a hybrid system. A parabolic trough collector is one of the concentrating systems capable of generating electricity on a large scale [7], as well as heating applications [8]. Parabolic trough collectors provide higher concentration levels compared to flat plate collectors

[*] Corresponding author: Tel: +603- 22463246, Fax: +603- 22463257
Email: khairulbuet@siswa.um.edu.my ; khairulbuet02@gmail.com (Attn: Md Khairul Islam)

RSC Advances Accepted Manuscript

[9]. System performance, which depends on design and material, is significantly influenced by factors such as mirror reflectivity, receiver absorptivity, heat transfer fluid and flow rate, tracking mechanism, and incident angle, among others [10]. Numerous studies on parabolic trough system that include its design and performance have been conducted. The least squares support vector machine method using numerical simulation demonstrated considerable success in modeling and optimizing the parabolic trough system [11]. Three-dimensional numerical simulation is similarly feasible and reliable in modeling parabolic trough systems [12]. According to Schmidt et al., the concentration ratio of receivers, which is notably high in a spherical receiver, suits paraboloidal reflectors with point focus and 90° rim angle [13]. Semi-cavity and modified cavity receivers investigated in a 65°-rim-angle paraboloidal dish indicate 70% to 80% steam conversion efficiency at 450 °C [14]. In a recent analytical model development for the optimum length of nanofluid-based volumetric solar receivers, the temperature in the steam power cycle reached up to 400 °C [15, 16]. An integrated combined-cycle solar power system using parabolic trough technique performs better than a conventional combined-cycle gas turbine power plant [17]. A concentrating system can produce steam to generate power through water (directly) or intermediate fluids. Intermediate heat transfer fluids significantly affect collector performance [18, 19]. The concentrating mechanism can attain different concentration levels and can be operated at various fluid temperatures. Fluid temperature rises once concentration ratio is increased, which heightens thermodynamic efficiency [20]. A parabolic trough concentrating solar system (PTCSS) can be designed for low/medium/high temperature applications. A smooth 90°-rim-angle fibreglass-reinforced parabolic trough collector for hot-water generation is designed and developed by [9]. A study on the design and construction of five parabolic trough solar collectors with various rim angles in a low-enthalpy process indicated 67% maximum efficiency and around 110 °C can be gained at 90° rim angle [21]. Another parabolic trough system with aperture 0.8 m, length 1.25 m, and rim angle 90^0 is developed with fiberglass as the reflector and copper tube as the solar ray absorber; it generates 75 °C hot water [9]. To measure

RSC Advances Accepted Manuscript

the performance coefficient of a refrigeration and cooling unit suitable for remote areas, a parabolic trough of aperture 1.26 m, aperture-to-length ratio 0.58, and rim-angle 90° are used in a particular research; it generated a maximum of 120 °C [22]. A solnova solar power station with 833 m^2-aperture 150 m-long parabolic collector generates 400 °C fluid temperature to produce power steam [23]. An analytical analysis on air-based cavity receiver for parabolic trough collector showed that it could achieve temperatures above 600 °C [24]. A pressurized air solar receiver is developed to generate power via gas turbine [25]. Recently, CO_2 has been considered as heat transfer fluid, and a number of research have been conducted on CO_2 based receiver [26-29]. A study on supercritical and transcritical CO_2 based central receiving system showed promising results [26]. However, the solar concentrating system has innate potentials in tropical regions where the higher diffusion of solar irradiation results in a higher temperature [30]. The application of PTCSS is feasible for absorption of refrigeration, hydrogen production, cooling of photovoltaic cells, and electricity generation [31-34].

This article is novel because of the development of a solar receiver for a parabolic trough concentrating solar system using carbon dioxide, nitrogen, and ammonia as heat transfer fluids, which are the basis of the comparative performance analysis. We aimed for this process because most studies have been conducted on liquid based solar receivers. However, liquid heat transfer fluids are limited in scaling and operating temperature ranges, whereas gases possess no such limitation. However, limited studies are made on gas-based receivers for concentrating system. To the best of the authors' knowledge, very few research have been done solely on CO_2 and on air-based receivers for parabolic trough collector. Moreover, no comparative performance analysis of the receiver for parabolic trough collector have been conducted using various gases. This paper aims to accomplish a comparative performance analysis and to optimize the receiver size of a parabolic trough concentrating solar system based on the carbon dioxide, nitrogen, and ammonia.

RSC Advances Accepted Manuscript

2. Methodology

2.1 Parabolic trough concentrating solar system

Parabolic trough is a kind of solar thermal collector, which is straight in one dimension, curved as a parabola in another, and constructed from polished metal mirror. Solar irradiation falling on the mirror is concentrated on the receiver along the focus line. The receiver tube contains a heat transfer fluid, which is heated to a high temperature by the concentrated solar irradiation. The hot fluid can be used for industrial and private purposes: electricity production, space heating, and hot water supply, among others. Figure 1 illustrates the system.

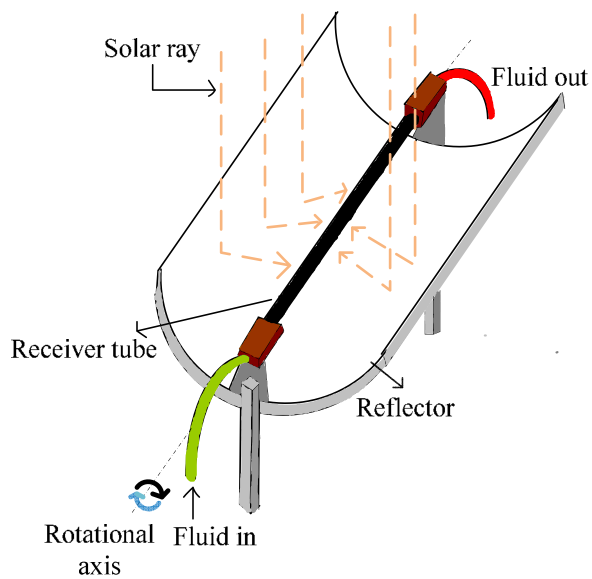

Figure 1. Parabolic trough concentrating solar system

2.2 Optical modeling

A parabolic trough system is oriented along the north–south horizontal axis at latitude 3.116° north of the equator and latitude 101°39$^{/}$59$^{//}$east of the prime meridian of Kuala Lumpur to track the sun's movement from east to west. Its incidence angle, θ can be calculated by using the following Equation [35, 36].

$$\theta = \cos^{-1}\left[\left(\cos^2\theta_Z + \cos^2\delta\sin^2\omega\right)^{\frac{1}{2}}\right] \tag{1}$$

where θ_Z, δ , and ω denote for zenith angle, declination, and hour angle, respectively.

RSC Advances Accepted Manuscript

The zenith angle can be calculated as:

$$\theta_Z = \cos^{-1}\left[\cos\phi\cos\delta\cos\omega + \sin\phi\sin\delta\right] \tag{2}$$

and declination as:

$$\delta = 23.45\sin\left(360\frac{284+n}{365}\right) \tag{3}$$

where n is the day of the year.

$(\tau\alpha)_b$ is the product of transmittance-absorptance for the beam radiation which can be calculated as [36].

$$(\tau\alpha)_b = \frac{\tau\alpha}{1-(1-\alpha)\rho_d} \tag{4}$$

where α, ρ_d, and τ denote the absorptance of the receiver, the cover reflectance for diffuse radiation, and the transmittance of the glass cover.

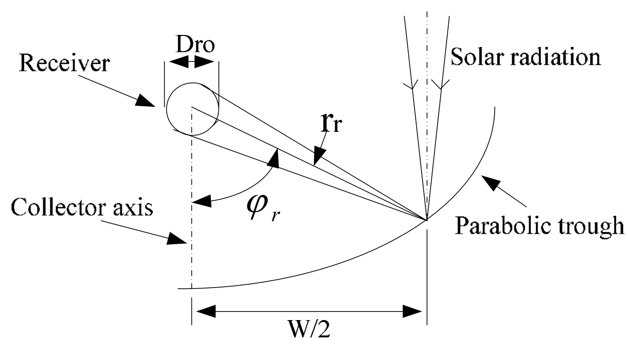

Figure 2 (a). Schematic diagram of a parabolic trough system

RSC Advances Accepted Manuscript

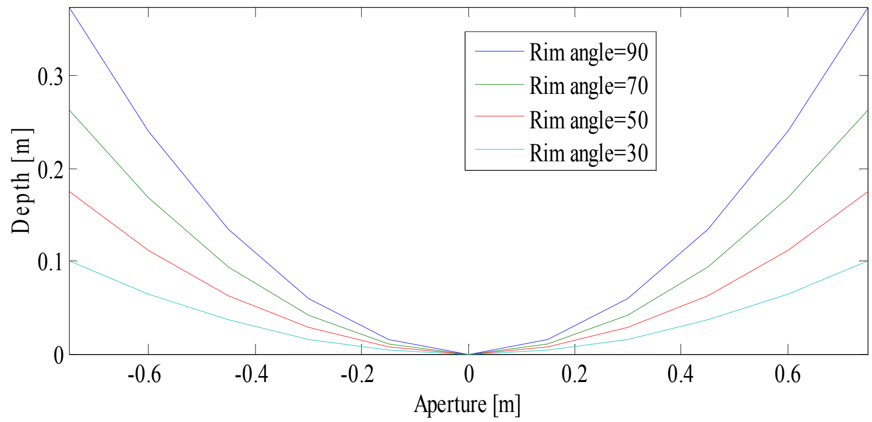

Figure 2(b). Profile of parabolic trough at various rim angles

2.3 Parabolic trough system design

The basic design parameters of a parabolic trough system are rim angle, trough aperture, and receiver size. The incident radiation at the rim of the collector (where the mirror radius R_r is maximum) establishes the rim angle. Rim angle plays a major role in the focal distance and image or the receiver size. Incident radiations emanating from the sun generally falls on the trough parallel. The trough focuses all the rays to the focal point and constructs a focal line. The receiver is placed concentrically along the focal line. Figure 2(a) is a schematic diagram of the parabolic trough.

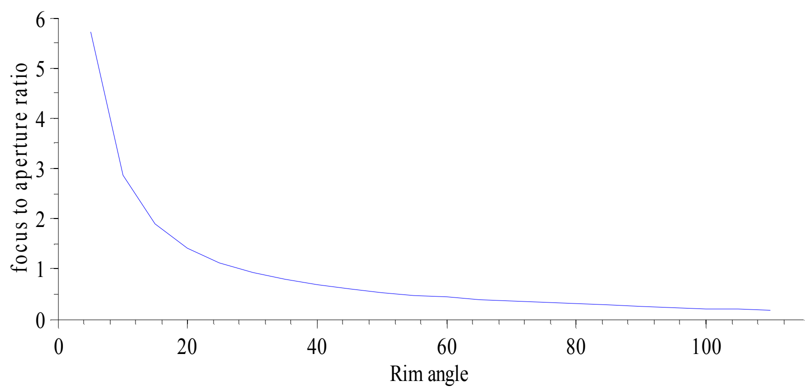

Figure 3. Ratio of focus-to-aperture versus rim angle

A parabolic trough system can be designed using the following equation:

$$y = ax^2 \tag{5}$$

RSC Advances Accepted Manuscript

where, $a = \frac{1}{4f}$.

$$\frac{f}{W} = 0.25\cot\frac{\varphi_r}{2} \qquad (6)$$

where f, W and φ_r denote the focus, width, and rim angle of the trough, respectively.

The focal point can be calculated by Equation (6) [35]. Trough profiles for the same aperture at various rim angles are as shown in Figure 2(b). Figure 3 plots focus-to-aperture ratio versus rim angle, where the increased rim angle is shown to decrease the focus-to-aperture ratio. Low focus-to-aperture ratio minimizes the spread of the reflected beam, resulting in less slope and reduced tracking errors. The concentration ratio is maximum at rim-angle 90°, which [37] provides a optimum intercept factor and a depth equal to the focal length. This study considers a 1.5 m-wide parabolic trough (an aluminum sheet with silver electroplating) and a 90° rim angle. The trough curvature length is calculated on Equation (7) [35].

$$T_{CL} = \frac{H_p}{2}\left\{\sec\frac{\varphi_r}{2}\tan\frac{\varphi_r}{2} + \ln\left[\sec\frac{\varphi_r}{2} + \tan\frac{\varphi_r}{2}\right]\right\} \qquad (7)$$

where T_{CL} is curvature length of the trough and H_p is the latus rectum of the parabola.

Afterwards, the receiver size is calculated on Equation (8).

$$CR = \frac{W - D_r}{\pi D_r} \qquad (8)$$

where CR is the concentration ratio, W is width of the trough, and D_r is the receiver diameter.

A simulation procedure is followed in designing an optimum receiver size. A concentration ratio (CR) is first assumed and then changed to calculate a different receiver diameter. Thermal analyses are then performed on different receiver sizes. The optimum receiver size is determined according to the collector maximum thermal efficiency, as calculated through Equation (9) [35, 36].

$$\eta_C = \frac{Q_u}{I_b A_a} \qquad (9)$$

RSC Advances Accepted Manuscript

where η_C, Q_u, I_b, and A_a denote collector thermal efficiency, useful heat gain, direct beam irradiation, and collector aperture area, respectively.

Useful heat (Q_u) gain can be calculated as [35, 36]:

$$Q_u = F_R\left[SA_a - A_r U_L\left(T_{fi} - T_a\right)\right] \tag{10}$$

where F_R, S, A_a, A_r, U_L, T_{fi}, and T_a refer to heat removal factor, absorbed radiation, collector aperture area, receiver area, heat loss coefficient, fluid temperature at inlet, and ambient temperature, respectively.

The solar energy flux absorbed by the receiver is calculated as [35, 36]:

$$S = I_b \rho_C \gamma (\tau\alpha)_b K\theta \tag{11}$$

where ρ_C, γ, $(\tau\alpha)_b$, and $K\ \Theta$ denote concentrator reflectance, intercept factor, transmittance-Absorptance product for beam radiation, and incidence angle modifier, respectively.

Incidence angle modifier can be calculated as:

$$K\theta = 1 - 6.74\times10^{-5}\theta^2 + 1.64\times10^{-6}\theta^3 - 2.51\times10^{-8}\theta^4 \tag{12}$$

Collector heat removal factor (F_R) significantly influence PTCSS performance, which can be calculated as [35, 36]:

$$F_R = \frac{m_f C_p}{U_L A_{r0}}\left[1 - e^{\left(\frac{-U_L F' A_R}{m_f C_P}\right)}\right] \tag{13}$$

where m_f, C_P, U_L, A_{ro}, and F' respectively denote fluid mass flow rate, specific heat capacity, heat loss coefficient, receiver outer area, and collector efficiency factor.

Collector efficiency factor, F' (which depends on the convective heat transfer coefficient, h_f besides the parabolic trough system dimensions) is calculated as [35, 36]:

$$F' = \frac{1}{U_L\left[\frac{1}{U_L} + \frac{D_{ro}}{D_{ri} h_f} + \left(\frac{D_{ro}}{2K_r}\ln\frac{D_{ro}}{D_{ri}}\right)\right]} \tag{14}$$

RSC Advances Accepted Manuscript

where D_{ro}, D_{ri}, and K_r respectively denote the outer and inner diameters, as well as the thermal conductivity of the receiver.

The heat transfer coefficient, h_f for fluids from receiver wall surface to fluids can be calculated by the following equation [38].

$$h_f = \frac{Nu_f . K_f}{D_{ri}} \tag{15}$$

where Nu_f and K_f refer to the Nusselt number and thermal conductivity of the fluid.

Nusselt number (Nu_f) can be calculated by standard tube flow equations. Laminar tube flow Nu_f is given as [39]:

$$Nu_f = 4.364 \tag{16}$$

where $Re_f <= 2300$.

For turbulent flow, Nu_f is as follows [38, 40]:

$$Nu_f = 0.023 \mathrm{Re}_f^{\ 0.8} \mathrm{Pr}_f^{\ 0.4} \tag{17}$$

where $2300 < Re_f < 1.25 \times 10^5$ and $0.6 < Pr_f < 100$.

or

$$Nu_f = 0.0214 \left(\mathrm{Re}_f^{\ 0.8} - 100 \right) \mathrm{Pr}_f^{\ 0.4} \tag{18}$$

where $10^4 < Re_f < 5 \times 10^6$ and $0.5 < Pr_f < 1.5$.

Here, Re is Reynolds number, Pr is Prandtl number, and subscript f is the fluid. Free convection occurs over the glass-cover tube. Free convective heat transfer is calculated as [41]:

$$Nu^{\frac{1}{2}} = 0.60 + 0.387 \left\{ \frac{Gr\,\mathrm{Pr}}{\left[1 + \left(0.559 / \mathrm{Pr} \right)^{9/16} \right]^{16/9}} \right\}^{1/6} \tag{19}$$

where $10^{-5} < \mathrm{GrPr} < 10^{12}$.

Grashof number, Gr is given as:

$$Gr = \frac{\beta \Delta T_g D_g^{\ 3}}{\nu^2} \tag{20}$$

RSC Advances Accepted Manuscript

where β, D_g, and ν denote the thermal conductivity temperature coefficient, glass tube diameter, and fluid kinematic viscosity, respectively.

A simulation program written in MATLAB optimizes the receiver size. The simulation uses three types of fluids, namely, ammonia, nitrogen, and carbon dioxide. The optimization procedure is outlined in the flow chart below.

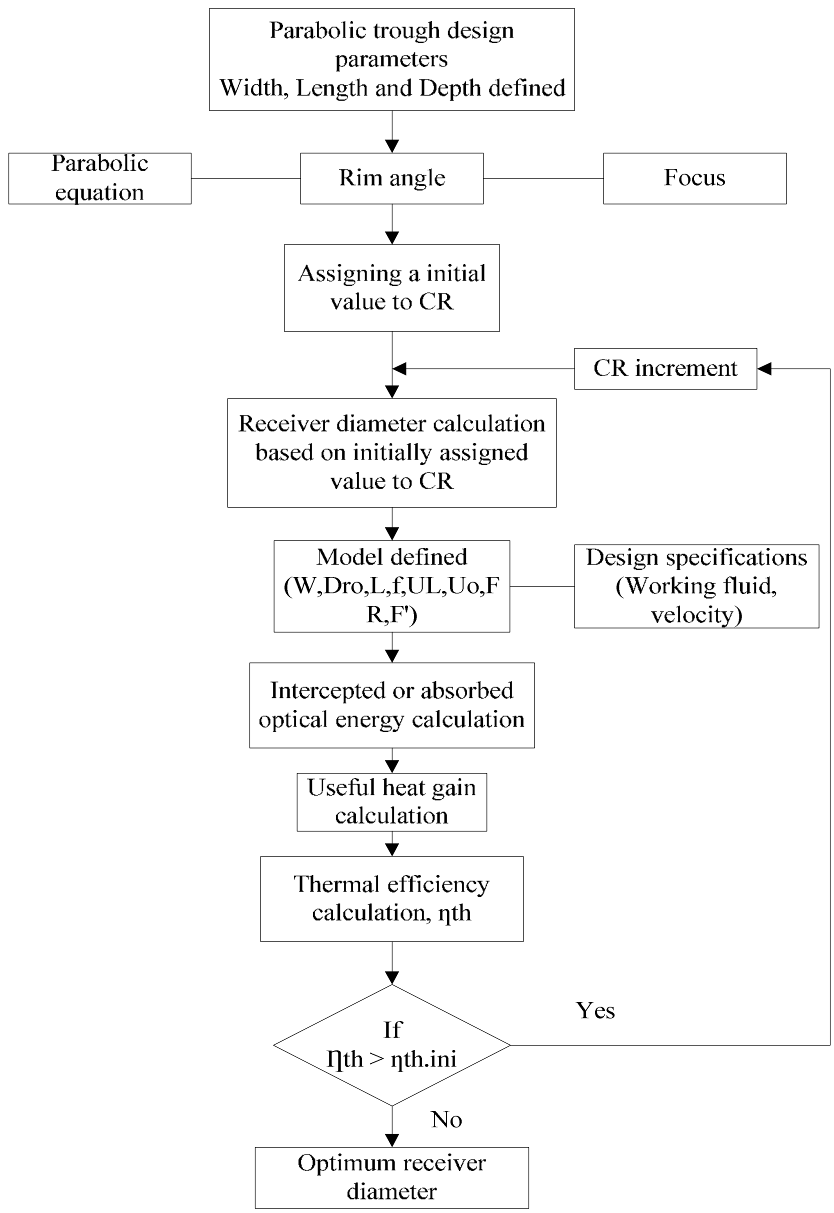

Figure 4. Outline of the procedure for optimizing the receiver size

RSC Advances Accepted Manuscript

3. Results and Discussion

The design optimization and overall system performance were investigated based on parameters that included the system thermal efficiency, useful heat gain, concentration ratio, heat removal factor, and mass flow rate of the heat transfer fluid. The speed of the three heat transfer fluids (ammonia, nitrogen, and carbon dioxide) was 18m/s. The effects of the CR and receiver diameter on the collector efficiency are presented in Figures 5(a) and 5(b).

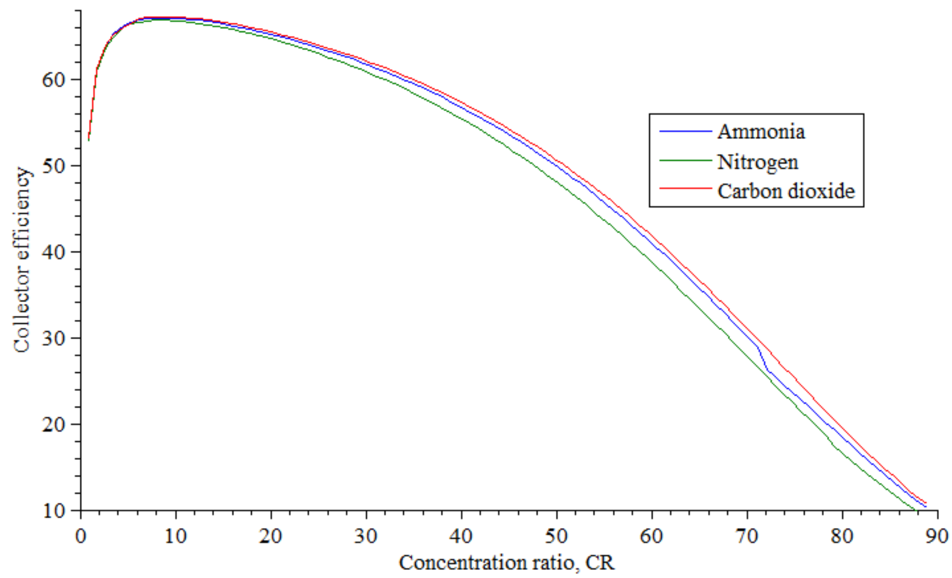

Figure 5(a). Effect of concentration ratio on collector efficiency

RSC Advances Accepted Manuscript

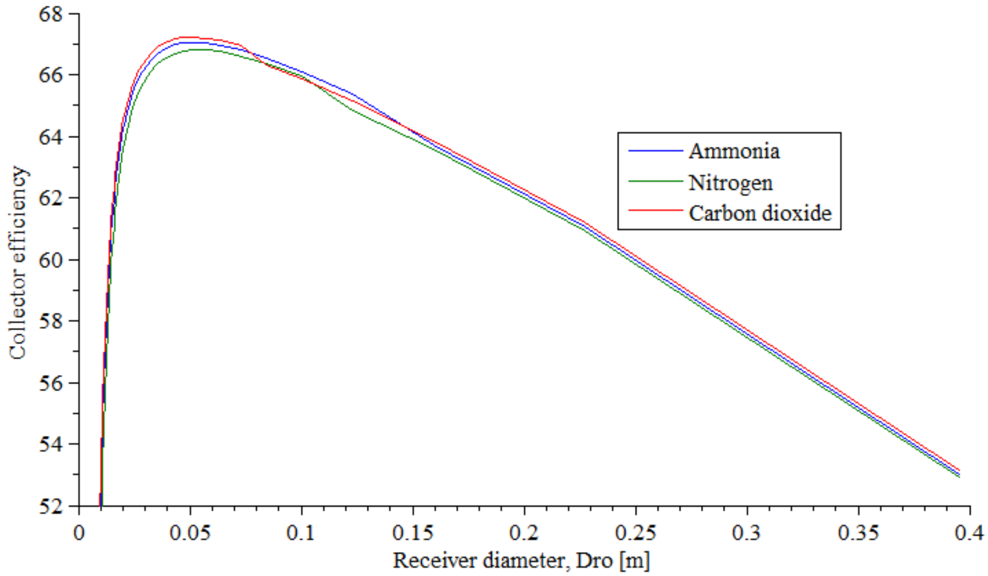

Figure 5(b). Effect of receiver sizes on collector efficiency

Figure 5(a) shows the initial increase of the collector efficiency across all the thermo fluids as CR increased, followed by its decrease when the maximum efficiency was reached at CR = 8.9. The maximum collector efficiency with each fluid occurred at CR = 8.9. Furthermore, Figure 5(b) shows rising collector efficiency with increasing receiver diameter, which reach the maximum at 51.8 mm (at CR = 8.9). The maximum efficiencies of ammonia, nitrogen, and carbon dioxide were 67.05%, 66.81%, and 67.22%, respectively. These values decreased when the receiver diameter increased. Both figures demonstrate similar increasing/decreasing rates.

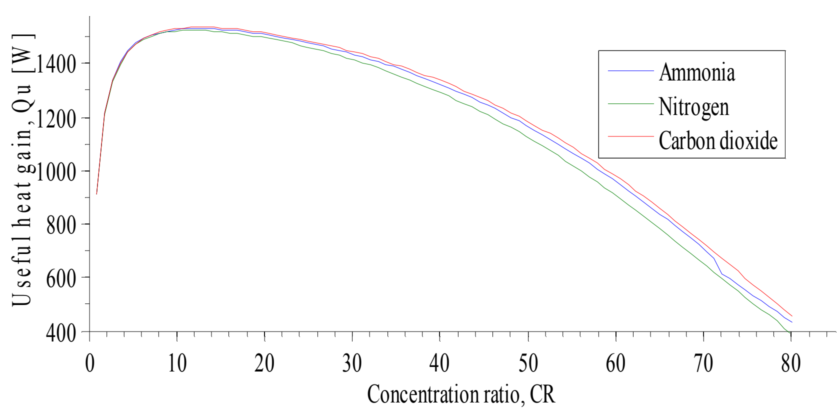

Figure 6(a). Effect of concentration ratio on useful heat gain

RSC Advances Accepted Manuscript

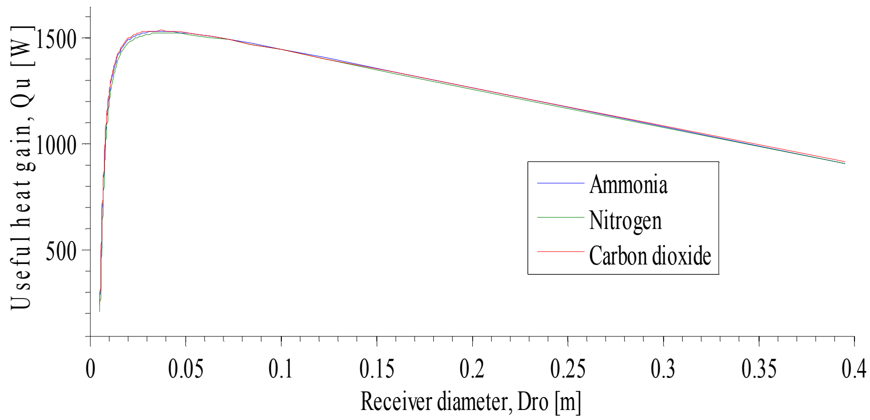

Figure 6(b). Effect of receiver sizes on useful heat gain

Figures 6(a) and 6(b) respectively present the effects of concentration ratio and receiver size on useful heat gain. These show that heat gain initially increases as CR or receiver size heightens before reaching the maximum value when CR was 10.8. Afterwards, the heat gain decreased although CR or receiver size increased. Both figures demonstrate that not all fluids affect useful heat gain. At CR=10.8, the collector efficiencies for ammonia, nitrogen, and carbon dioxide were 64.43%, 64.02%, and 64.67% respectively, which are all lower than the maximum efficiencies.

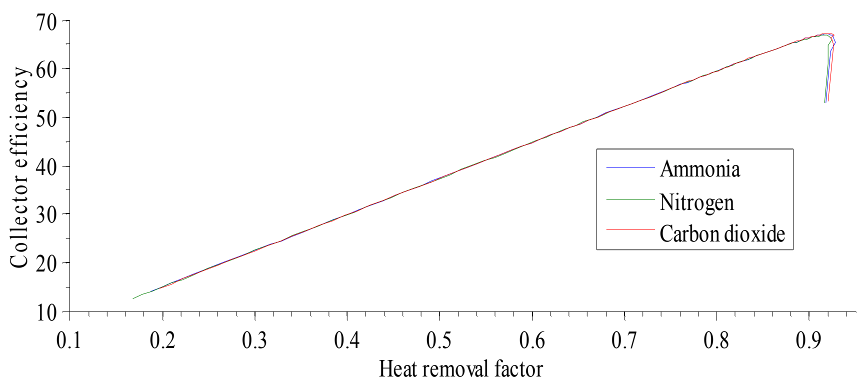

Figure 7. Effect of heat removal factor on collector efficiency

A co-relation between heat removal factor and collector efficiency was observed. Heat removal factor is a dimensionless parameter that indicates the thermal energy transfer characteristic of the collector and the effect of fluid convective heat transfer on the collector thermal performance. Figure 7 shows efficiency increasing linearly with rising heat removal. Among the heat removal

RSC Advances Accepted Manuscript

factors of 0.9206, 0.9184, and 0.9150 (for carbon dioxide, ammonia and nitrogen respectively), collector efficiency diminished across all the fluids. Collector efficiencies for carbon dioxide, ammonia, and nitrogen, are found to be maximum against the above mentioned heat removal factors at 67.22%, 67.05%, and 66.81%, respectively.

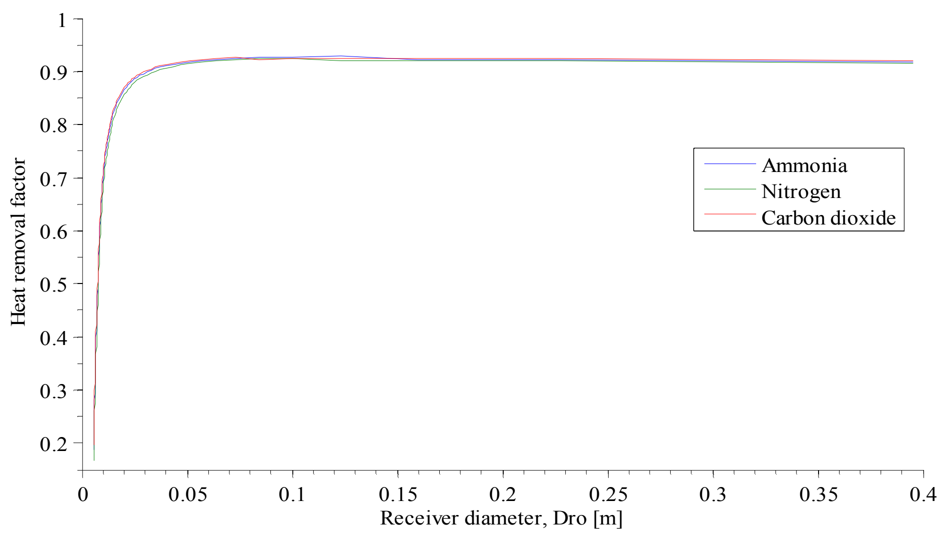

Figure 8. Effect of receiver size on heat removal factor

Figure 8 shows the effect of receiver size on heat removal factor. Furthermore, it demonstrates an increasing heat removal factor when receiver size increased. However, the value is almost constant for all fluids at or over the receiver diameter 51.8 mm. Heat removal factor is a function of fluid mass flow rate. Figure 9 shows its effect on heat removal factor. The heat removal factor of each fluid increased as the fluid mass flow rate rose. The increasing rates are similar across all the fluids, up until a 0.91 heat removal factor. After that the increase rates start varies slowly. Upon reaching the maximum values (i.e., 0.928 at 0.119 kg/s for ammonia, 0.927 at 0.102 kg/s for carbon dioxide, and 0.925 at 0.146 kg/s for nitrogen), the heat removal factors suddenly dropped and slowly decreased after minimal increases. The collector efficiency factor is mainly responsible for changing the heat removal factor. With increasing fluid mass flow rate, the collector efficiency factor increases up to 0.933, suddenly falls to 0.926, and then slowly decreases. Diminishing rates differed across all the fluids. The decrease rate for ammonia was

RSC Advances Accepted Manuscript

higher compared to the other two fluids. Also notable was the difference of the maximum mass flow rates among the fluids because of the changing diameters of the receiver and fluid density.

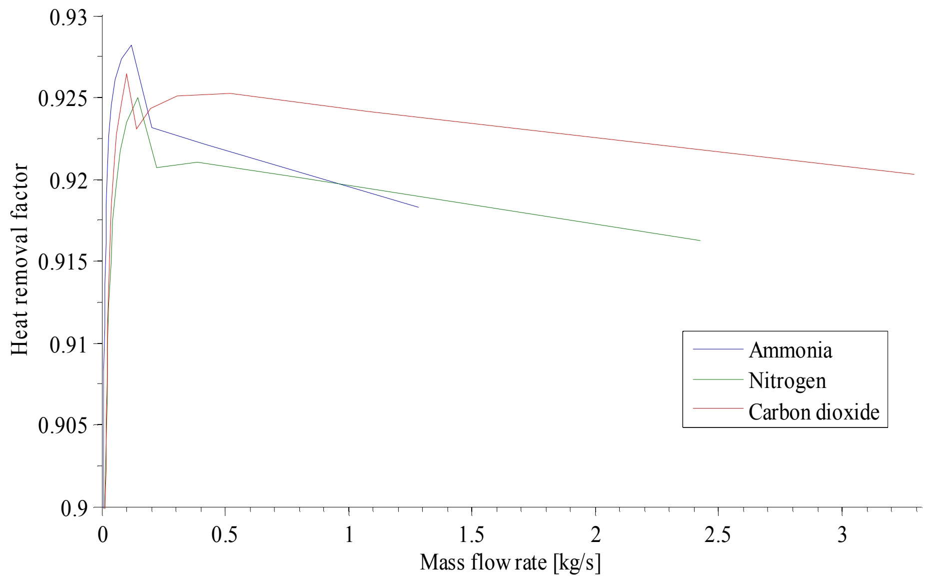

Figure 9. Effect of fluid mass flow rate on heat removal factor

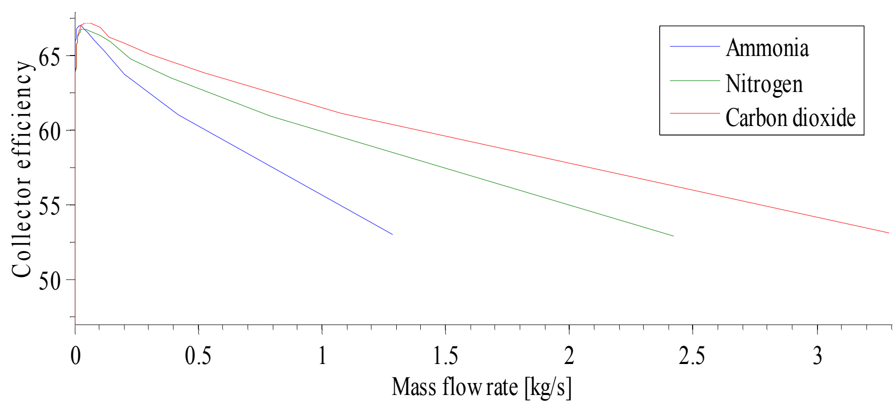

Figure 10. Effect of fluid mass flow rate on the collector efficiency

Figure 10 shows an increasing collector efficiency when fluid mass flow rate increased with a maximum (67.22%, 67.05% and 66.81%) at the mass flow rates of 0.0491 kg/s, 0.0192 kg/s, and 0.0362 kg/s for carbon dioxide, ammonia, and nitrogen, respectively. Afterwards, efficiency decreased when the mass flow rate increased, with differing decrease rates (higher in ammonia than in nitrogen or carbon dioxide). Heat removal factor is a function of mass flow rate, specific

RSC Advances Accepted Manuscript

heat, heat loss coefficient, receiver outer area, and collector efficiency factor. Furthermore, a relation among heat removal factor, heat gain, collector aperture area, receiver size, and collector efficiency is noted as well. Fluid mass flow rate increases as receiver size rises. Increases in receiver size, decreases the aperture area which causes the decrement of heat gain. Thus, although increment of heat removal factor influences collector efficiency positively, the continuous decrement of aperture area decreases heat gain, and collector efficiency could ultimately increase up to the heat removal factors of 0.9206, 0.9184, and 0.9150 (for carbon dioxide, ammonia, and nitrogen, respectively). Here, it is also notable that change of mass flow rate is not the same for all fluids. Thus, at the same aperture area of 2.836 m^2, different mass flow rates (0.0491 kg/s, 0.0192 kg/s, and 0.0362 kg/s, for carbon dioxide, ammonia, and nitrogen, respectively) provide maximum collector efficiencies such as 67.22%, 67.05%, and 66.80%.

4. Conclusion

The influence of parameters such as heat removal factor, collector efficiency factor, mass flow rate, and collector aperture area on collector thermal efficiency were investigated. Three fluids, namely, carbon dioxide, ammonia, and nitrogen, were used for the analysis. The optimum receiver size (diameter) (producing the highest efficiency) was found at 51.8 mm for the concentrator of 1.5 m aperture and 2 m length. Maximum collector efficiencies are 67.22%, 67.05% and 66.81% at the same aperture area 2.836 m^2 occurred with different mass flow rates 0.0491 kg/s, 0.0192 kg/s, and 0.0362 kg/s for carbon dioxide, ammonia, and nitrogen, respectively.

Acknowledgement

The authors acknowledge the financial support of the High Impact Research Grant (HIRG) scheme (Project No: UM.C/HIR/MOHE/H-16001-00-D000032, Campus Network Smart-Grid System for Energy Security) for this research.

RSC Advances Accepted Manuscript

References

[1]. M.A. Abdullah, A.P. Agalgaonkar, K.M. Muttaqi, Climate change mitigation with integration of renewable energy resources in the electricity grid of New South Wales. Australia, *Renew. Energy*, 2014, **66**: 305-313.

[2]. M. Hasanuzzaman, N.A. Rahim, M. Hosenuzzaman, R. Saidur, I.M. Mahbubul, M.M. Rashid, Energy savings in the combustion based process heating in industrial sector. *Renew. Sust. Energ. Rev.,* 2012, **16**(7): 4527-4536.

[3]. D. Kaya, Renewable energy policies in Turkey. *Renew. Sust. Energ. Rev.*, 2006, **10**: 152-163.

[4]. F. Ahmed, A.Q. Al Amin, M. Hasanuzzaman, R. Saidur, Alternative energy resources in Bangladesh and future prospect. *Renew. Sust. Energ. Rev.*, 2013, **25**: 698-707.

[5]. M. Schroeder, Utilizing the clean development mechanism for the deployment of renewable energies in China. *Appl. Energy*, 2009, **86**(2): 237-242.

[6]. R. Saidur, T.C. Meng, Z. Said, M. Hasanuzzaman, A. Kamyar, Evaluation of the effect of nanofluid-based absorbers on direct solar collector. *Int. J. Heat Mass Transf.*, 2012, **55**: 5899-5907.

[7]. F. Lippke, Direct steam generation in parabolic trough solar power plants: numerical investigation of the transients and the control of a once through system. *J. Sol. Energy Eng.*, 1996, **118**: 9-14.

[8]. S. Kalogirou, Parabolic trough collectors for industrial process heat in Cyprus. *Energy*, 2002, **27**: 813-830.

[9]. A.V. Arasu, T. Sornakumar, Design, manufacture and testing of fiberglass reinforced parabola trough for parabolic trough solar collectors. *Sol. Energy*, 2007, **8**(10): 1273-1279.

[10]. K.S. Reddy, K.R.K. Solar collector field design and viability analysis of stand-alone parabolic trough power plants for Indian conditions. *Energy Sustain Dev.*, 2012, **16**(4): 456–470.

RSC Advances Accepted Manuscript

[11]. Q. Liu, M. Yang, J. Lei, H. Jin, Z. Gao, Y. Wang, Modelling and optimizing parabolic trough solar collector systems using the least squares support vector machine method. *Sol. Energy*, 2012, **86**(7): 1973-1980.

[12]. Z.D. Cheng, Y.L. He, F.Q. Cui, R.J. Xu, Y.B. Tao, Numerical simulation of a parabolic trough solar collector with nonuniform solar flux conditions by coupling FVM and MCRT method. *Sol. Energy*, 2012, **86**(6): 1770-1784.

[13]. G. Schmidt, P. Schmid, H. Zewen, S. Moustafa, Development of a point focusing collector farm system. *Sol. Energy*, 1983; **31**: 299-311.

[14]. N.D. Kaushika, K.S. Reddy, Performence of a low cost solar paraboloidal dish steam generating system. *Energy conv. Manag.*, 2000, **41**: 713-726.

[15]. A. Veeraragavan, A. Lenert, B. Yilbas, S. Al-Dini, E.N. Wang, Analytical model for the design of volumetric solar flow receivers. *Int. J. Heat Mass Transf.*, 2012, **55**(4): 556-564.

[16]. A. Fernández-García, E. Zarz, L. Valenzuel, M. Pérez, Parabolic-trough solar collectors and their applications. *Renew. Sust. Energ. Rev.*, 2010, **14**(7): 1695–1721.

[17]. A.R. Montes, M. Muñoz, J.M. Martínez-Val, Performance analysis of an Integrated Solar Combined Cycle using Direct Steam Generation in parabolic trough collectors. *Appl. Energy,* 2011, **88**(9): 3228–3238.

[18]. Z.D. Cheng, Y.L.H., F.Q. Cui, R.J. Xu, Y.B. Tao, Numerical simulation of a parabolic trough solar collector with nonuniform solar flux conditions by coupling FVM and MCRT method. *Sol. Energy*, 2012, **86**(6): 1770-1784.

[19]. M.M. Billah, M.M. Rahman, U.M. Sharif, N.A. Rahim, R. Saidur, M. Hasanuzzaman, Numerical analysis of fluid flow due to mixed convection in a lid-driven cavity having a heated circular hollow cylinder. *Int. Commun. Heat Mass Transf.*, 2011, **38**(8): 1093-1103.

[20]. R.V.D. Barlev, P. Stroeve, Innovation in concentrated solar power. *Sol. Energy Mater. Sol. Cells*, 2011, **95**(10): 2703–2725.

RSC Advances Accepted Manuscript

[21]. O.A. Jaramillo, E. Venegas-Reyes, J.O. Aguilar, R. Castrejon-Garcia, F. Sosa-Montemayor, Parabolic trough concentrators for low enthalpy processes. *Renew. Energy*, 2013, **60**: 529-539.

[22]. N.H. Abu-Hamdeh, K.A. Alnefaie, K.H. Almitani, Design and performance characteristics of solar adsorption refrigeration system using parabolic trough collector: Experimental and statistical optimization technique. *Energy conv. Manag.*, 2013, **74**: 162-170.

[23]. SPS, www.nrel.gov/csp/solarpaces/project_detail.cfm/projectID=25, （accessed june 2013).

[24]. P. Matarrese, A. Gaetano, S. Airaghi, D. Montorfano, M.C. Barbato, G. Ambrosetti, A. Pedretti, Performance analysis of a novel air-based cavity receiver. *Energy Procedia*, 2014, **49**:438-446.

[25]. P. Pozivil, V. Aga, A. Zagorskiy, A. Steinfeld, A pressurized air receiver for solar-driven gas turbines. *Energy Procedia*, 2014, **49**: 498-503.

[26]. R. Chacartegui, J.M. Munoz de Escalona, D. Sanchez, B. Monje, T. Sanchez, Alternative cycles based on carbon dioxide for central receiver solar power plants. *Appl. Therm. Eng.*, 2011, **31**(5): 872-879.

[27]. D.J. Chapman, D.A. Arias, An assessment of the supercritical carbon dioxide cycle for use in a solar parabolic trough power plant. Proceedings of SCCO, Power Cycle Symposium 2009.

[28]. Z. Ma, C.S. Turchi, Advanced supercritical carbon dioxide power cycle configurations for use in concentrating solar power systems, Supercritical CO_2 Power Cycle Symposium 2011.

[29]. S. Rajinesh, A.M. Sarah, S.R. Andrew, A.J. Peter, Dynamic characteristics of a direct-heated supercritical carbon-dioxide Brayton cycle in a solar thermal power plant. *Energy*, 2013, **50**: 194-204.

[30]. S. Pramuang, R.H.B. Exell, Transient test of a solar air heater with a compound parabolic concentrator. Renew. *Energy*, 2005, **30**(5): 715-728.

RSC Advances Accepted Manuscript

[31]. M.T. Lee, M. Werhahn, D.J. Hwang, N. Hotz, R. Greif, D. Poulikakos, C.P. Grigoropoulos, Hydrogen production with a solar steam methanol reformer and colloid nanocatalyst. *Int. J. Hydrog. Energy*, 2010, **35**: 118-126.

[32]. M. Hammad, S. Habali, Design and performance study of a solar energy powered vaccine cabinet. *Appl. Therm. Eng.*, 2000, **20**(18): 1785-1798.

[33]. A. Akbarjadeh, T. Wadowski, Heat pipe based cooling system for photovoltaic cells under concentrated solar radiation. *Appl. Therm. Eng.*, 1996, **16**(1): 81-87.

[34]. K. Kaygusuz, Prospect of concentrating solar power in Turkey: The sustainable future. *Renew. Sust. Energ. Rev.*, 2011, **15**(1): 808-814.

[35]. JA. Duffie, W. Beckman, *Solar engineering of thermal processes*. 2nd ed. New york: John Wiley & Sons, Inc.; 1991.

[36]. S.A. Kalogirou, *Solar energy engineering: Processes and Systems*. Elsevier's Science & Technology, UK; 2009.

[37]. V. Arora, a.S.T. Development and Performance Characteristics of a Low-Cost Parabolic Solar Collector, *International Conference on Power and Energy Systems* (ICPES 2012) 2012, **56**:80-84.

[38]. Y. Cengel, *Heat and mass transfer-a practical approach*. 3rd ed. Tata Mcgraw-Hill; 2007.

[39]. R.K. Shah, A.L. London, Laminar flow: Forced convection in ducts. New york: Academic Press; 1978.

[40]. V. Gnielinski, New equations for heat and mass transfer in turbulent pipe and channel flow. *In Chem. Eng.*, 1976, **16**: 359-368.

[41]. S.W. Churchill, H.H.S. Chu, Correlating equations for laminar and turbulent free convection from a horizontal cylinder. *Int. J. Heat Mass Transf.*, 1975, **18**: 1049-1053.

RSC Advances Accepted Manuscript